

PACS 29.90.+r

INVESTIGATION OF NaI(Tl) SCINTILLATORS FOR POSITRON-EMISSION TOMOGRAPH AT HIGH GAMMA-QUANTUM INTENSITIES

O.G. Konovalov, S.T. Lukyanenko, A.A. Zybalov

National Science Center "Kharkov Institute of Physics and Technology", Kharkov 61108, Ukraine

E-mail: afanserg@kipt.kharkov.ua

Received January 9, 2004

The characteristics of NaI(Tl) scintillators for positron-emission tomograph (PET) were investigated at high photon intensities and different photomultiplier tube pulse durations in the single-channel mode as well as in the coincidence mode. Comparative analysis has shown that main characteristics of NaI(Tl) crystals are not inferior to those of Bi₄Ge₃O₁₂ crystals (BGO). The results of investigations evidence on the possibility for manufacturing a cost-effective PET on the basis of NaI(Tl) scintillators with the performances at a level of advanced PETs with BGO crystals.

KEY WORDS: photon, scintillator, positron-emission tomograph (PET), energy discrimination, energy and spatial resolution, random and true coincidences, counting rate, clipped pulse.

Over the past several years, advances in positron-emission tomography (PET) instrumentation and positron-emitting radiopharmaceuticals have enabled scientists and clinicians to perform a wide range of research and clinical studies of human physiology. Detailed information about the functional state of patient's internals and their structural singularities can be obtained by introduction of positron-active radionuclides into his body. Early diagnostics of a tumour is provided by recording the space-time distributions of the arising γ -radiation field. For these investigations the most widely applied radionuclides are ¹¹C (T=20.4 min), ¹³N (T=9.96 min), ¹⁵O (T=2.07 min), ¹⁸F (T=109.7 min) (T is the half period) [1]. For reconstruction of a 3-D image of an object under study it is necessary to accumulate the statistic data on positron annihilation in this object at a level of 10^6 to 10^8 events according to the stated diagnostic problems. A PET detecting system is capable to count every event in the mode of coincidence of two annihilation photons. Therefore for statistic data accumulation within the time interval T (the half period) it is necessary to use radionuclides with a sufficiently high activity and systems operating at high-counting rates. For brain imaging the radionuclide activity up to ~ 5 mCi is permissible and for dynamic heart imaging it can reach 20 mCi. The total γ -radiation intensity in the PET detecting system is $\sim 3 \cdot 10^8$ and $\sim 1.2 \cdot 10^9$ photon/s, respectively.

For effective event counting at a high γ -radiation intensity one needs, first of all, "fast" scintillators with a short luminescence decay time ($\tau \sim 6-30$ ns). They are scintillators of a YAP, PWO, BaF₂, CeF₃ type and other [1]. However, each of them has some disadvantages, for example: low light yield, low density, or complex and expensive procedure of crystal growing. In this connection, today, for new PETs designing one uses, for the most part, comparatively "slow" Bi₄Ge₃O₁₂ ($\tau \sim 300$ ns) and NaI(Tl) ($\tau \sim 240$ ns) scintillators. Bi₄Ge₃O₁₂ (BGO) scintillators are more widely applied in PETs for photon detection due to their advantages of density ($\rho = 7.13$ g/cm³) and effective charge ($Z_{\text{eff}} = 74$) over NaI(Tl) scintillators ($\rho = 3.67$ g/cm³, $Z_{\text{eff}} = 50$).

The present PETs based on BGO are the compact multidetector and multiannular systems comprising, in total, $\sim 10-12$ thousands of detectors connected with a computer-assisted multichannel electronic system [2]. Such a PET configuration allows significant decreasing of the photon-irradiation intensity of each of detectors. On the whole, the present PETs are very complex detecting electronic instruments to a value of several millions of dollars.

At present, one carries on a search of the more cost-effective PET schemes. As an alternative approach for a PET is to use a few large-area NaI(Tl) detectors (6 or 8) mounted along the perimeter of a ring [3]. The opposite pairs of detectors are connected to the circuits of double coincidences. Each of detectors works as an Anger scintillation camera without a collimator [4,5]. With such a PET scheme it is possible to decrease significantly the total number of detectors, electronics units and the cost of PETs. For development of such PET it is necessary to carry out detailed investigations on the characteristics of NaI(Tl) crystals with different sizes under conditions of real photon intensities, and it is the goal of our work.

The first PET with large-area NaI(Tl) detectors was manufactured in the University of Pennsylvania (Philadelphia, USA) [3,6]. It comprises six crystals of $500 \times 150 \times 25$ mm³. It is interesting to compare its performance with that of multidetector PETs regarding the following characteristics: spatial and energy resolution, efficiency of annihilation photon detection, maximum counting rate of true and random coincidences.

The spatial resolution of advanced PETs with BGO crystals is varying from 2.8 mm to 4.5 mm in the PET centre [7] and can be improved due to decreasing the transversal dimensions of BGO crystals. At the same time, the number of detectors and electronics units should be increased for the total counting rate be remained. These improvements, however, are accompanied by an increase in cost of the instrument. The spatial resolution of a PET with large-area

NaI(Tl) scintillation crystals is determined by the crystal thickness, as in the case when an Anger gamma camera is used [4,5]. The spatial resolution of the first PET with NaI(Tl) scintillators (25 mm thick) is 5.2 mm. It is two times worse in comparison with the better specimens of PETs with BGO crystals. The energy resolution of PETs with BGO crystal is 27-30 % for 511 keV γ -quantum and that of the PETs with NaI(Tl) large-area scintillators is 10 % [3,6]. The efficiency of 511 keV photon detection in PETs with BGO crystals (25-30 mm thick) is 90-100 %, and in PETs with NaI(Tl) scintillators (25 mm thick) it is 56 %. However, the detection efficiency of PETs with BGO decreases to 65 % because of the edge effects and gaps between the crystals [6]. In the case of double coincidences the efficiency of PETs with BGO crystals is 42 % and with NaI(Tl) scintillators it is 31 %, i.e. the difference is insignificant.

One of the main problems for PETs is to increase the counting rate of true coincidences and to decrease the contribution of random coincidences. The counting rate of the first PETs with large-area NaI(Tl) scintillators is only 100 kcps [3,6] against 500 kcps of the PETs with BGO crystals (50 % contribution of random coincidences). The spatial resolution and the counting rate of a PET with large-area NaI(Tl) scintillators can be improved by decreasing, first of all, the crystal thickness, by increasing the geometric efficiency of a PET and by clipping the pulses at the photomultiplier tube (PMT) output. The operation speed of a detecting system can be increased taking into account the great advantage of the NaI(Tl) scintillator over the BGO crystal, namely, the light yield. For this the technique with photomultiplier pulses clipping is to be used.

The spatial resolution Δx of the NaI(Tl) scintillator for absorption of 511 keV photons was calculated by the model of [8]. The measurements of [9,10] show that, indeed, the spatial resolution can be improved from 5-6 to 3.5-4 mm by decreasing the scintillator thickness from 25 to 18 mm. The results are in accordance with the most known values of Δx for PETs with BGO crystals. However, the counting rate of photons with $E_\gamma=511$ keV decreases from 56 to 44 % and in the case of double coincidences from 30 to 20 %. The decrease of the efficiency as a result of NaI(Tl) crystal thickness decreasing can be compensated at the expense of the increased geometric efficiency. The value of the latter in the present PETs with BGO crystals is only 1 % (100 % correspond to 4π sr) [11]. It can be much higher when a whole-body annular NaI(Tl) scintillator of a cylindrical form (diameter ~400 mm, length ~250 mm) is applied for PETs.

METHOD

The above considerations shows that it is possible to design a cost-effective PET based on NaI(Tl) scintillators with performances corresponding to the better models of PETs with BGO crystals. For development of a such PET scanner it is necessary to study the characteristics of different NaI(Tl) scintillators under conditions of real photon intensities used for brain imaging. The detailed investigations will enable to choose the most optimum geometric dimensions of a PET scanner and to determine operating conditions of the electronic system for event counting (pulse time length, operation speed, background event discrimination etc.). Fig. 1. schematically presents the electronic instrumentation used for investigation of various specimens of NaI(Tl) scintillators.

The NaI(Tl) scintillator was irradiated with photons from a radioactive source ^{137}Cs and a positron-active source ^{22}Na . The forming delay line was used for pulse clipping at the PMT output. PMT pulses were amplified and discriminated by means of CAMAC electron blocks (models 1501 and 1202). Pulse coincidences were measured using the circuit of coincidences having the time resolution of 25 ns and the scaler PS-15 [12].

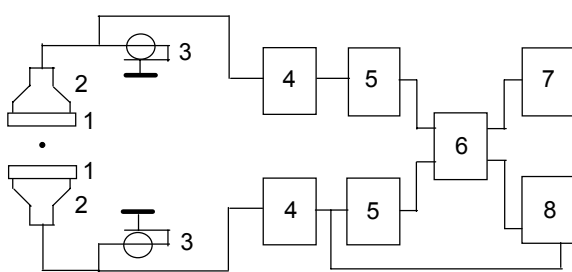


Fig. 1. Block-diagram of the electronics:

- 1 – scintillator, 2 – spectrometric PMT-118, 3 – forming delay line,
- 4 – amplifier, 5 – discriminator, 6 – circuit of coincidences,
- 7 – scaler, 8 – pulse analyzer.

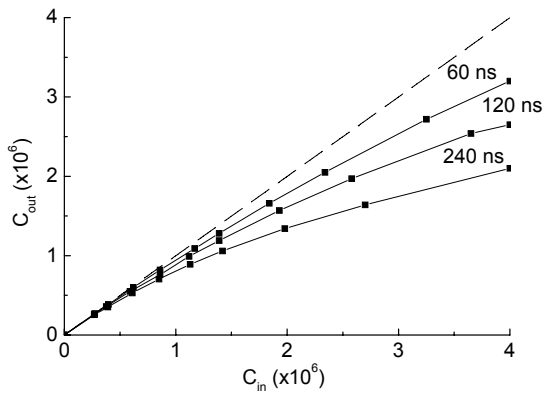


Fig. 2. The measured single-channel output counting rate as a function of the input counting rate for the clipped pulses $t=240, 120, 60$ ns.

RESULTS

Single-channel detector counting rate measurements

These measurements were carried out at different intensities of the NaI(Tl) scintillator irradiation with photons from the source ^{137}Cs using the clipped PMT pulses of 240, 120, 60 ns and the minimum discrimination of 140 keV.

Fig. 2 presents the measured counting rates C_{out} at the single-channel output as a function of the input counting rate C_{in} . The effective width of clipped input pulses for the NaI(Tl) scintillator ($40 \times 40 \text{ mm}^2$) was $t=240, 120, 60 \text{ ns}$. The dashed straight line corresponds to the pulse counting efficiency of 100 % at the electronic channel output. Under real conditions this level of counting is realized only at comparatively inferior counting rates at the channel input ($C_{\text{in}} < 2 \cdot 10^4 \text{ cps}$) with the given pulse duration. As the counting rate C_{in} increases, the loss in the counting rate C_{out} increases too because of a dead time of the electronic channel which is determined by the effective width t of every input pulse ($C_{\text{out}} = C_{\text{in}} e^{-C_{\text{in}} t}$) [13]. The losses in the pulse counting rate are 38 % and 21 % for $t=120 \text{ ns}$ and 60 ns with $C_{\text{in}} = 4 \cdot 10^6 \text{ cps}$. The permissible activity of radionuclides used for brain imaging is 5 mCi that determines the maximum counting rate of $2.5 \cdot 10^6 \text{ cps}$ in the single-channel input [3,6]. The counting rate losses are 24 % and 14 % at the pulse duration $t=120 \text{ ns}$ and 60 ns .

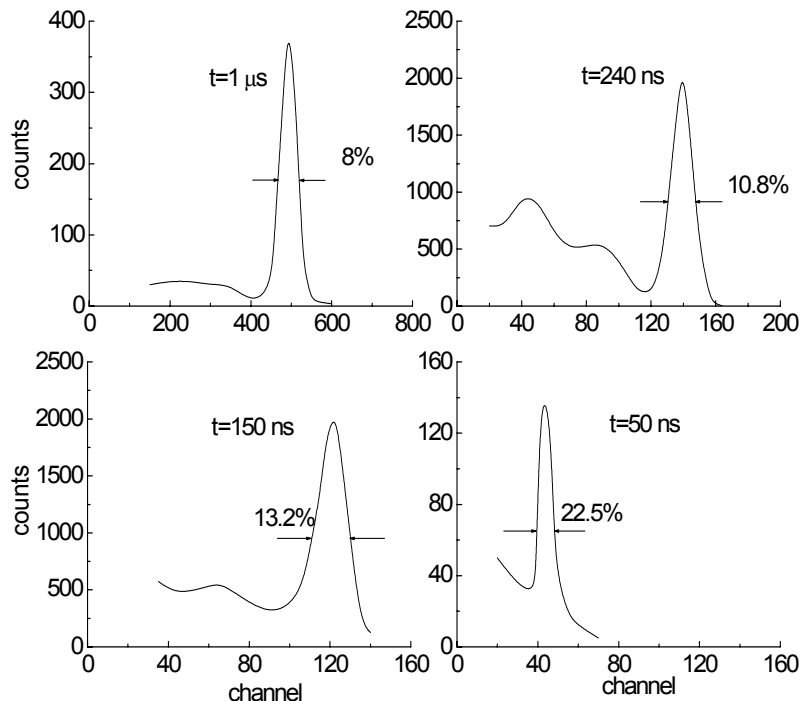


Fig. 3. Energy spectra of photons with $E=661 \text{ keV}$ for the NaI(Tl) scintillator ($40 \times 40 \text{ mm}^2$) at a low counting rate (10^3 cps) for pulses of $1 \mu\text{s}$, 240 ns , 150 ns , 50 ns duration.

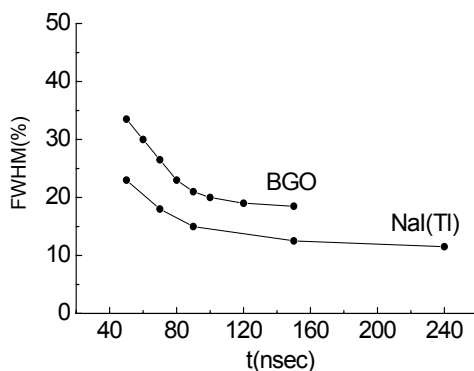


Fig. 4. FWHM (%) energy resolution of the NaI(Tl) and BGO scintillators (the ^{137}Cs source) as a function of pulse duration (ns). Data for NaI(Tl) are ours; data for BGO are taken from [14].

of Compton scattering. As the level of discrimination increases and at $E_d=580 \text{ keV}$ it is completely noticeable. In Fig. 5 shown is the Gaussian distribution of detected photons in the photopeak (dashed line). FWHM of this distribution is 31 %. This resolution can be improved by differential discrimination of the photopeak. Thus the contribution of the noninformative Compton part of the spectrum and overlapping effects are decreased by 37 %.

Energy spectra

The measurements of the energy spectra give an important information about performances of different scintillators used for detection of photons of low and high intensities. Fig. 3 presents the energy spectra of 661 keV photons for the NaI(Tl) scintillator at a low counting rate and different pulse duration. The measurement results show that as pulses are clipped from $1 \mu\text{s}$ to 50 ns , the energy resolution is changing from 8 % to 22.5 % and remains sufficiently effective to distinguish the photopeak in the photon energy spectrum.

The FWHM (full width half maximum) energy resolution of NaI(Tl) and BGO scintillators at different pulse durations is shown in Fig. 4. The energy resolution was measured on the BGO crystal used for detection of high-energy photons [14]. The crystal was in the form of a truncated pyramid of

24 cm length with the rectangular bases of $6.5 \times 5.5 \text{ cm}^2$ and $1.2 \times 1.9 \text{ cm}^2$. We measured the energy resolution on the NaI(Tl) scintillator of $40 \times 40 \text{ mm}^2$ at a lower counting rate and a minimum discrimination. The FWHM energy resolution of the NaI(Tl) scintillator is 14 % against 20 % for the BGO crystal with the pulse duration $t=100 \text{ ns}$. The energy resolution of a PET with BGO crystals having small transverse dimensions (4-6 mm) is 27-30 % for $t=300 \text{ ns}$. The decrease in $\Delta E/E$ is caused by the presence of appreciable edge effects increasing the amplitude spread of photons being detected.

Fig. 5 presents the energy spectra of 661 keV photons for the NaI(Tl) scintillator ($40 \times 40 \text{ mm}^2$) at a high counting rate and different levels of discrimination. The shift of the photopeak due to the pulse overlapping at a high counting rate of $1.4 \cdot 10^6 \text{ cps}$ is observed. At the minimum level of discrimination the left part of the photopeak is almost completely overlapped by the spectrum

In fig. 6 the photon energy spectra for the NaI(Tl) scintillator ($30 \times 25 \text{ mm}^2$) at different levels of energy discrimination are presented. The maximum counting rate with clipped pulses of 150 ns and the minimum discrimination (140 keV) is $0.7 \cdot 10^6$ cps. The decrease of the NaI(Tl) scintillator thickness from 40 to 25 mm improves the energy resolution from 31 % to 19 %.

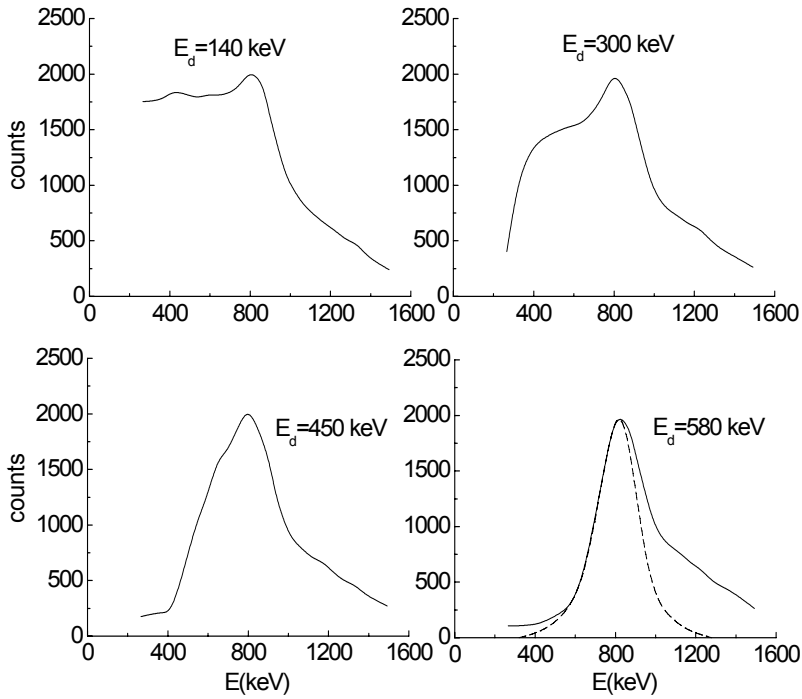


Fig. 5. The energy spectra of photons with $E=661 \text{ keV}$ for NaI(Tl) scintillator ($40 \times 40 \text{ mm}^2$) for the energy discrimination of 140, 300, 450 and 580 keV.

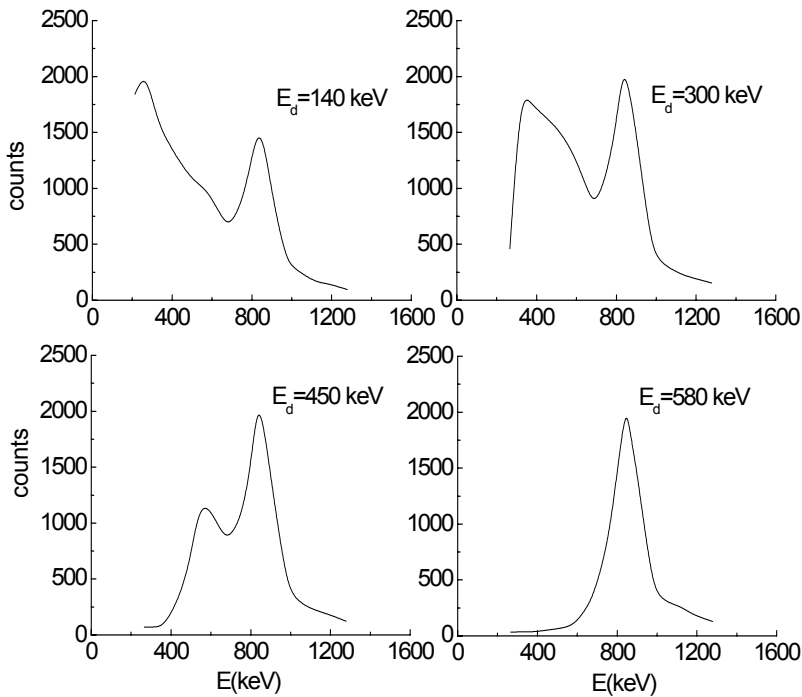


Fig. 6. The energy spectra of photons with $E=661 \text{ keV}$ for NaI(Tl) scintillation ($30 \times 25 \text{ mm}^2$) for the energy discrimination of 140, 300, 450 and 580 keV.

agreement with the measurement data is observed only for the source ^{22}Na .

So, the results of measurements of true and random coincidences, for one pair of NaI(Tl) scintillators at high photon intensities and counting rates of $\sim 10^6$ cps in the each channel, evidence on the possibility for detection of $\gamma\gamma$ -coincidences at a counting rate of $8 \cdot 10^4$ cps with the random coincidence contribution of 50 %.

Counting rates characteristics of photon coincidences

The electronics used for measurement of the true and random coincidences is schematically presented in fig.1. The annihilation photons of the ^{22}Na source are detected by two NaI(Tl) scintillators ($40 \times 40 \text{ mm}^2$). The time resolution of the coincidence circuit is 25 ns. The maximum counting rates of the clipped pulses of 150 and 100 ns in each of channels of the coincidence circuit were 10^5 and $1.1 \cdot 10^5$ cps, respectively. The measured counting rates of true coincidences are $2.3 \cdot 10^4$ and $2.7 \cdot 10^4$ cps for these pulse time lengths. The contribution of random coincidences is 3 %. Under real conditions of imaging the brain the latter is considered as a distributed field of annihilation photon sources. The maximum intensity of the irradiation of each large-area NaI(Tl) scintillator can reach $2 \cdot 10^6$ cps in this field [3]. The main part of detected photons is given by the background events from the pair of opposite scintillators in the PET.

In the present work we used ^{137}Cs as a source of background events. This source irradiated, simultaneously with the source ^{22}Na , both crystals NaI(Tl). The total counting rate of clipped pulses of 150 ns and 100 ns from $^{22}\text{Na} + ^{137}\text{Cs}$ in each of channels of the circuit of coincidences was $0.9 \cdot 10^6$ and 10^6 cps, respectively. The maximum counting rate of coincidences was $6.5 \cdot 10^4$ and $8.2 \cdot 10^4$ cps for 60 % and 55 % contribution of random coincidences, respectively for these pulse time lengths. The counting rate of true coincidences was $2.5 \cdot 10^4$ and $3.2 \cdot 10^4$ cps. Good

CONCLUSION

The results of investigations of NaI(Tl) crystals at high photon intensities permit to conclude the following.

The high light yield of the NaI(Tl) scintillators provides a possibility for detection of γ -radiation of radionuclides with the clipped pulses of a duration up to 50-60 ns. In the single-channel detector mode the maximum counting rate of these pulses reaches $4.2 \cdot 10^6$ cps. The loss in the counting rate is 21 %.

The FWHM energy resolution of the photopeak of 661 keV photons with the 50 ns clipped pulses is 22 %, as compared to 35 % in the case of a BGO crystal. Thus, it is possible to measure the $\gamma\gamma$ -coincidences at higher intensities of irradiation of the NaI(Tl) scintillator. However, it is necessary to carry out investigations of the NaI(Tl) scintillators with the pulse time length of 50-60 ns at high intensities of photon irradiation.

The energy discrimination provides a reliable separation of a photopeak from a noninformative part of the spectrum under conditions of high intensities of irradiation of NaI(Tl) scintillators.

The estimations of the spatial resolution of NaI(Tl) scintillators with a different thickness, performed in the framework of the model described in [8], have shown that the use of scintillators 18 mm in thickness gives the resolution of 0.35-0.4 mm that is at a level of the better values for the present PETs with BGO crystals.

The results of investigations evidence that it is possible to manufacture a cost-effective PET with NaI(Tl) scintillators possessing the performances of advanced multidetector PETs with BGO crystals. A promising version of such a tomograph can be a PET developed on the basis of a whole-body cylindric NaI(Tl) scintillator [15]. This cost-effective PET with a small number of PMTs and units of electronics can provide a high level of patient study. Moreover, the PETs with NaI(Tl) crystals are successfully used in the clinical brain study. One of the most prominent specimens of PETs of this class is a S-PET scanner operating in the PET-center of Pennsylvania [9].

We are grateful to Prof. P.Sorokin for his helpful discussion and comments.

REFERENCES

1. John L. Humm et al. From PET detectors to PET scanners // European Journal of Nuclear Medicine and Molecular Imaging.-2003.-V. 30. - №11.-P. 1574-1597.
2. R. Timothy et al. Performance Characteristics of a Whole-Body PET Scanner // Journ. Nucl. Med.-1994.-V. 35. -№8.-P. 1398-1406.
3. J.S. Karp et al. Performance of a position sensitive scintillation detectors // Phys. Med. Biol.-1985.-V. 30.-P. 643-655.
4. H.O. Anger. Scintillation camera // Rev. Sci. Instrum.-1958.-V. 29.-P. 27-33.
5. S.D. Kalashnikov. Physical fundamentals of designing scintillation gamma-chambers. Moscow: Energoatomizdat, 1985.-121 p. (in Russian).
6. J.S. Karp et al. Event localization in a continuous scintillation detector using digital processing // IEEE Transact. Nucl. Sci.-1986.-V. 33.-№1.-P. 550-555.
7. S. Pavlopoulos et al. Design and Performance Evaluation of a High-Resolution Small Animal Positron Tomograph // IEEE Transact. Nucl. Sci.-1996.-V. 43.-№6.-P. 3249-3255.
8. H.O. Anger et al. Gamma-Ray Detection Efficiency and Image Resolution in Sodium Iodide // Rev. Sci. Instrum.-1964.-V. 35.-№6.-P. 693-697.
9. Lars-Eric Adam et al. Performance of a Whole-Body PET Scanner Using Curve-Plate NaI(Tl) Detectors // Journal of Nuclear Medicine.-2001.-V.42.-№12.-P.1821-1830.
10. R. Freifelder et al. Design and Performance of the HEAD PENN-PET Scanner // IEEE Transact. Nucl. Sci.-1994.-V. 41.-№4.-P. 1436-1440.
11. J.S. Karp et al. Positron Emission Tomography with a Large Axial Acceptance Angle: Signal-to-Noise Considerations // IEEE Nucl. Sci. Symp.-1990.-V. 2.-P. 1228-1235.
12. V.F. Chechetenko, Yu.P. Antufiev, P.V. Sorokin. Pereschetnaya sistema PS-15. Kharkov, Preprint KIPT 70-31.-1970 (in Russian).
13. D.A. Mankoff et al. The high count rate performance of a two-dimensionally position-sensitive detector of positron emission tomography // Phys. Med. Biol.-1989.-V. 34.-№4.-P. 437-456.
14. G. Gervino et al. Study on BGO resolution with clipped photomultiplier pulses // NIM.-1991.-A309.-P. 497-499.
15. J.S. Karp et al. Three-Dimensional Imaging Characteristics of the HEAD PENN-PET Scanner // Journ. Nucl. Med.-1997.-V. 38.-№4.-P. 636-643.

ИССЛЕДОВАНИЕ СЦИНТИЛЯТОРОВ NaI(Tl) ДЛЯ ПОЗИТРОН-ЭМИССИОННОГО ТОМОГРАФА ПРИ ВЫСОКИХ ИНТЕНСИВНОСТЯХ ГАММА-КВАНТОВ

О.Г. Коновалов, С.Т. Лукьяненко, А.А. Зыбалов

ННЦ «Харьковский физико-технический институт», Академическая 1, Харьков 61108, Украина

E-mail: afanserg@kipt.kharkov.ua

Исследованы характеристики сцинтиляторов NaI(Tl) для позитрон-эмиссионного томографа (ПЭТ) при высоких интенсивностях γ -квантов и разных длительностях импульсов с фотоэлектронных умножителей как в одноканальном, так и в режиме совпадений. Сравнительный анализ с кристаллами $\text{Bi}_4\text{Ge}_3\text{O}_{12}$ (BGO) показал, что по основным характеристикам NaI(Tl) не уступает BGO. Всё это свидетельствует о возможности создания ПЭТ на основе сцинтиляторов NaI(Tl) с параметрами, соответствующими лучшим моделям ПЭТ с кристаллами BGO, но по стоимости значительно ниже.

КЛЮЧЕВЫЕ СЛОВА: фотон, сцинтилятор, позитрон-эмиссионный томограф, энергетическая дискриминация, энергетическое и пространственное разрешение, случайные и истинные совпадения, скорость счёта, укороченный импульс